New Insight into Cycloidal Areas

Tom M. Apostol and Mamikon A. Mnatsakanian

doi:10.4169/193009709X458573

1. INTRODUCTION. A *cycloid* is the path traced by a point on the boundary of a circular disk that rolls without slipping along a straight line. It forms a sequence of arches resting on the line, as shown in Figure 1. It is known that the area of the shaded region below one arch is three times the area of the rolling disk. Our analysis shows that the factor 3 reflects a much deeper property of cycloidal sectors. Figure 2 shows various stages of rotation of the disk, together with *cycloidal sector OPC* bounded by arc *OP* and two line segments *OC* and *PC*. At each stage we have:

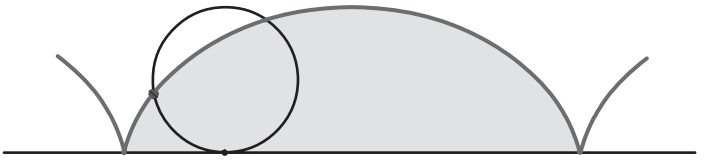

Figure 1. Cycloidal arch has area three times that of the rolling disk.

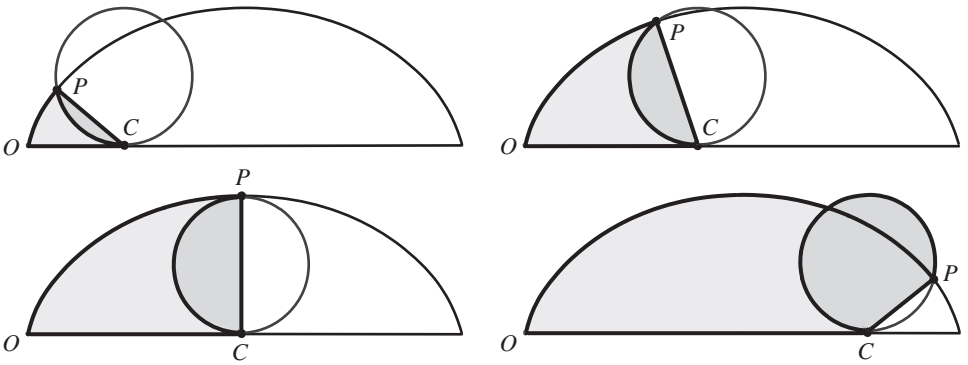

Figure 2. Each cycloidal sector *OPC* has area three times that of the shaded segment of the rolling disk cut by chord *PC*, where *C* is the contact point of the disk and base line.

Theorem 1. *Cycloidal sector OPC has area three times that of the overlapping circular segment cut from the rolling disk by chord PC.*

This remarkable geometric property follows easily from an elegant area relation illustrated in Figure 3. The rolling disk is tangent to the upper and lower boundaries of the rectangle circumscribing the cycloid, at corresponding points of tangency T and C. Diameter TC divides the rolling circle into two semicircles, one of which intersects the cycloid at point P as indicated. The line segment joining P and T cuts off a portion PCT of the rolling disk that we call a *wedge*. We call region $PODT$, bounded by cycloidal arc PO and line segments OD, DT, and TP, a *cycloidal cap*. The key that unlocks Theorem 1 is the following surprising relation:

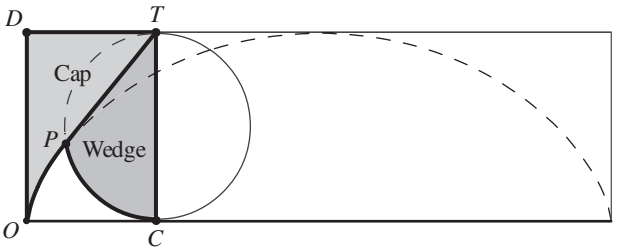

Figure 3. Cycloidal cap *PODT* has the same area as wedge *PCT* of the rolling disk.

Lemma 1. *Cycloidal cap PODT has the same area as wedge PCT of the rolling disk.*

The foregoing area relations are extended to epicycloids and hypocycloids in Section 4.

2. AREA OF CYCLOIDAL CAP (PROOF OF LEMMA 1). Lemma 1 will be deduced as a consequence of Mamikon's sweeping-tangent theorem ([**1**, p. 26], [**2**, p. 900], [**4**]) which states that the area of a tangent sweep is equal to that of its corresponding tangent cluster (see Section 7). First we show that each chord *PT* is tangent to the cycloid at point *P*. This will show that as the disk rolls to the position shown in Figure 4, the tangent segment from the cycloid to the upper horizontal boundary of the rectangle, starting initially at *OD*, sweeps out cycloidal cap *PODT*.

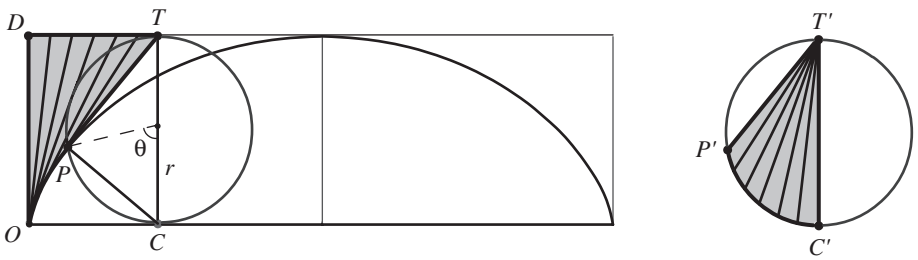

Figure 4. Cycloidal cap is a tangent sweep with the same area as tangent cluster $T'C'P'$.

To see that *PT* is tangent to the cycloid at *P*, note that triangle *TPC* is inscribed in the semicircle with diameter *TC* and hence is a right triangle. Now we observe a fundamental property of the rolling disk. Because it rolls along the horizontal line without slipping, its point of contact *C* is instantaneously at rest, and point *P* undergoes instantaneous rotation about *C* with *PC* as instantaneous radius of rotation. This is called the *instantaneous rotation principle*, illustrated in Figure 5 for a region bounded by a convex closed curve that rolls without slipping along a fixed curve Γ. The line segment joining an arbitrary point *P* of the region to the point of contact *C* with Γ is *normal* to the path of *P*. Equivalently, a line through *P* perpendicular to *PC* (shown in Figure 5 with arrows) is *tangent* to the path of *P*. This principle is evident for a polygon rolling about a vertex, and it also holds for all curves that are limits of polygons.

Apply the instantaneous rotation principle to the disk that generates the cycloid in Figure 4. Because angle *TPC* is a right angle, chord *PT* is perpendicular to normal *PC* and hence is tangent to the cycloid. Thus, the cycloidal cap is a tangent sweep.

To form the corresponding tangent cluster $T'C'P'$, translate each chord *PT* (parallel to itself) by moving all extremities *T* to one point T' on the right of Figure 4. Then

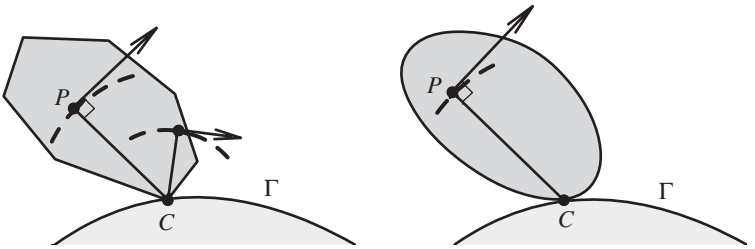

Figure 5. Instantaneous rotation principle. Point P undergoes instantaneous rotation about point of contact C, so PC is normal to the path of P.

the other extremities P move to various points P'. Thus each segment $P'T'$ is equal in length and parallel to the corresponding chord PT. Obviously, segments $P'T'$ are chords of a circular disk congruent to the rolling disk. By Mamikon's theorem, the area of tangent sweep $PODT$ is equal to that of tangent cluster $T'C'P'$. This tangent cluster is congruent to the wedge TCP of the rolling disk in Figure 3, and we obtain Lemma 1.

3. AREA OF CYCLOIDAL SECTOR (PROOF OF THEOREM 1). Throughout this paper we employ square brackets to designate areas of regions. Thus, in Figure 6 we use the following notations:

[Sector] = area of cycloidal sector OPC in Figures 2 and 6b.

[Tusk] = area of tusk-like curvilinear region OPC below the cycloid and the disk (unshaded in Figure 6a).

[Wedge] = area of wedge PCT of the circular disk (darker shading in Figure 6a).

[Segm] = area of the segment of the disk cut off by chord PC (darker shading in Figure 6b).

[Tri] = area of right triangle TPC in Figure 6b.

[Rect] = area of rectangle $ODTC$.

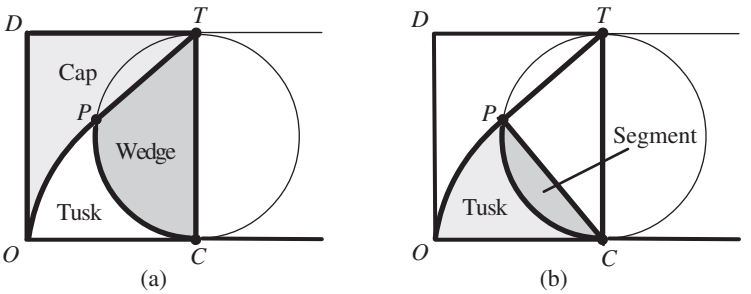

Figure 6. (a) Rectangle $ODTC$ is the union of Cap, Wedge, and Tusk. (b) Cycloidal sector OPC is the union of Tusk and Segment.

Theorem 1 states that

$$[\text{Sector}] = 3[\text{Segm}]. \tag{1}$$

Figure 6b reveals that [Sector] = [Segm] + [Tusk]; hence (1) is equivalent to

$$[\text{Tusk}] = 2[\text{Segm}].$$

Now by Lemma 1 the area of cap $PODT$ equals [Wedge], and from Figure 6a we find

$$[\text{Tusk}] = [\text{Rect}] - 2[\text{Wedge}] = [\text{Rect}] - 2[\text{Segm}] - 2[\text{Tri}], \tag{2}$$

where we used the relation

$$[\text{Wedge}] = [\text{Segm}] + [\text{Tri}]. \tag{3}$$

In Figure 4, OD has length $2r$, and OC has the length $r\theta$ of circular arc CP, so

$$[\text{Rect}] = (2r)(r\theta) = 4\left(\frac{1}{2}r^2\theta\right). \tag{4}$$

From Figure 4 we see that $\frac{1}{2}r^2\theta$ is the area of the central sector of the disk with central angle θ, which is also equal to $[\text{Segm}] + \frac{1}{2}[\text{Tri}]$. Therefore (4) implies

$$[\text{Rect}] = 4[\text{Segm}] + 2[\text{Tri}]. \tag{5}$$

When this is used in the right side of (2), we obtain $[\text{Tusk}] = 2[\text{Segm}]$, which proves Theorem 1. Thus, the area of a cycloidal sector is reduced to that of a segment of the rolling disk, which is given by the elementary formula

$$[\text{Segm}] = \frac{r^2}{2}(\theta - \sin\theta), \tag{6}$$

obtained by subtracting the area of the isosceles triangle with base PC in Figure 4 from the area of the circular sector with central angle θ.

Since the edge PC of any cycloidal sector POC is normal to the cycloid, as we observed in our discussion of instantaneous rotation, we see that sector POC is, in fact, swept by a moving segment normal to the cycloid.

4. EPICYCLOIDAL AND HYPOCYCLOIDAL CAP AND SECTOR. Instead of rolling a circular disk along a fixed line we now roll it along the circumference of a fixed circle. Then a point on the boundary of the rolling disk traces a more general type of cycloid, called a *hypocycloid* if the disk rolls internally to the fixed circle, with the two centers on the same side of the common tangent as in Figures 7a and 7b, or an *epicycloid* if it rolls externally, with the centers on opposite sides of the common tangent as in Figures 7c and 7d. The shape will depend on the radius r of the rolling disk compared to the radius R of the fixed circle. In Figure 7a, $r = R/4$ and the hypocycloid is called an *astroid*. In Figure 7b, $r = R/3$ and the hypocycloid is called a *deltoid*. The epicycloid in Figure 7c is a *nephroid* ($r = R/2$), and in Figure 7d it is a *cardioid* ($r = R$). The cycloid in Figure 1 is the limiting case $R \to \infty$.

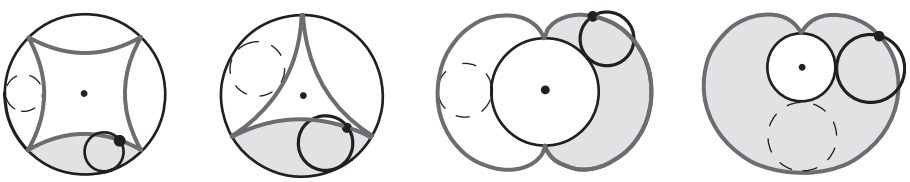

(a) astroid (b) deltoid (c) nephroid (d) cardioid

Figure 7. Examples of hypocycloids (a) and (b), and epicycloids (c) and (d).

We extend Theorem 1 to both epicycloids and hypocycloids (Figure 8) by replacing the factor 3 by a new constant independent of the position of the rolling disk. In what follows, we assume that $r \le R/2$ for hypocycloids, which entails no loss in generality because of a double generation theorem of Daniel Bernoulli that ensures that the same family of epicycloids and hypocycloids is generated when $r > R/2$. The extended result is:

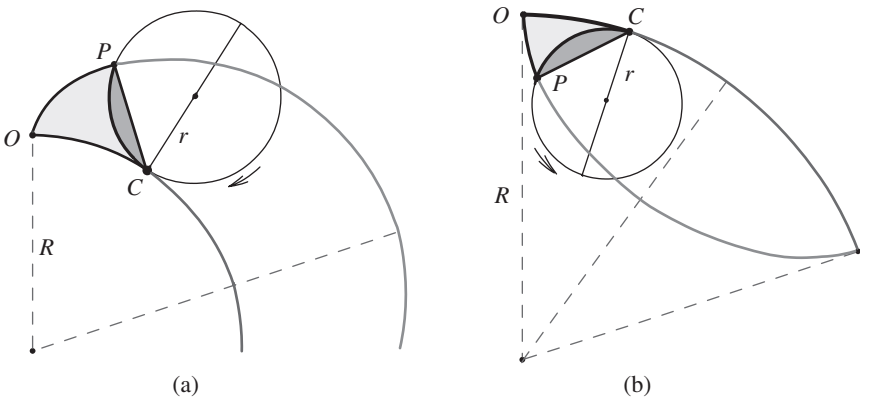

Figure 8. Sector *POC* has area $\omega_\pm$ times that of the overlapping circular segment cut off by chord *PC*.

Theorem 2. *Any epicycloidal or hypocycloidal sector OPC has area $\omega_\pm$ times that of the overlapping segment of the rolling disk cut by chord PC, with $\omega_+ = 3 + 2r/R$ for the epicycloid, and $\omega_- = 3 - 2r/R$ for the hypocycloid.*

We will deduce Theorem 2 from Lemma 2, an extension of Lemma 1. In Lemma 1 the cycloidal cap *PODT* and wedge *PCT* have equal areas, but in Lemma 2 (illustrated for an epicycloid in Figure 9a) these areas are related as follows:

Lemma 2. *Cycloidal cap PODT has area $\kappa_\pm$ times that of wedge PCT of the rolling disk, with $\kappa_+ = 1 + 2r/R$ for the epicycloid, and $\kappa_- = 1 - 2r/R$ for the hypocycloid.*

Proof of Lemma 2. We treat the epicycloid first. Figure 9a shows an epicycloidal arc *OP* traced by point P on a disk of radius r as it rolls along the outer circumference of a fixed circle of radius R. The epicyloid lies inside the annular ring between the fixed

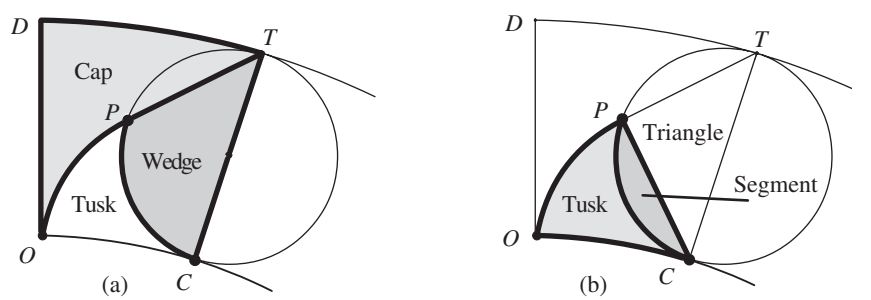

Figure 9. (a) Ring *ODTC* is the union of epicycloidal Cap, Wedge, and Tusk. (b) Epicycloidal sector *OPC* is the union of Tusk and Segment.

circle of radius R and the concentric circle of radius $R + 2r$. This ring plays a role similar to that of the rectangle circumscribing the cycloid in Figure 3.

Now refer to Figure 10a. Point P, initially at O, traces portion OP of the epicycloid. The point of contact of the two circles, also initially at O, moves through angle φ to point C as shown, tracing circular arc OC of length $R\varphi$. Circular arc CP of radius r has length $r\theta$, where θ is the central angle in the rolling circle, as shown. Rolling takes place without slipping so the two arclengths CP and OC are equal:

$$r\theta = R\varphi. \tag{7}$$

A line through the two centers intersects the outer circle at its point of tangency T with the rolling circle. Triangle TPC is inscribed in a semicircle of diameter CT, so angle TPC is a right angle. Point C serves as center of instantaneous rotation of the rolling circle, so segment PC is normal and segment PT is tangent to the epicycloid. As the tangent moves from its initial position OD to that shown in Figure 10a, it sweeps out the cycloidal cap $PODT$, turning through angle

$$\alpha = \beta + \varphi. \tag{8}$$

Here β is the inscribed angle PTC subtending arc PC, and is half of central angle θ. From (7) we have $\varphi = r\theta/R = 2\beta r/R$, hence (8) becomes

$$\alpha = \kappa_+ \beta, \tag{9}$$

where $\kappa_+ = 1 + 2r/R$. Now form a tangent cluster by translating each tangent segment PT (parallel to itself) so point T moves to a fixed point T' in Figure 10b. By Mamikon's theorem, the area of the tangent sweep in Figure 10a is equal to that of the tangent cluster shaded in Figure 10b. The length of segment PT is equal to $2r \cos \beta = 2r \cos(\alpha/\kappa_+)$, and therefore this tangent cluster can be compressed to form the circular wedge in Figure 10c by rotating each translated tangent $P'T'$ about T' to decrease the

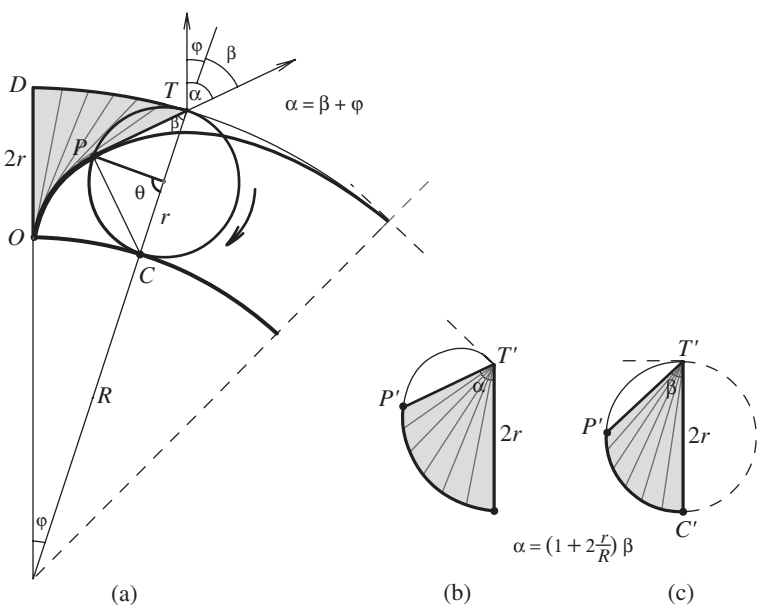

Figure 10. Proof of Lemma 2 for an epicycloidal sector.

angle α by a factor of κ_+, from α to $\alpha/\kappa_+ = \beta$. The area of the cluster is therefore equal to that of the circular wedge multiplied by κ_+. But wedge $T'C'P'$ in Figure 10c is congruent to wedge TCP of the rolling disk in Figure 10a, so this proves Lemma 2 for the epicycloid. A similar proof works for a hypocycloidal cap $PODT$ in Figure 11a. In this case $\alpha = \beta - \varphi$, giving us $\kappa_- = 1 - 2r/R$. ∎

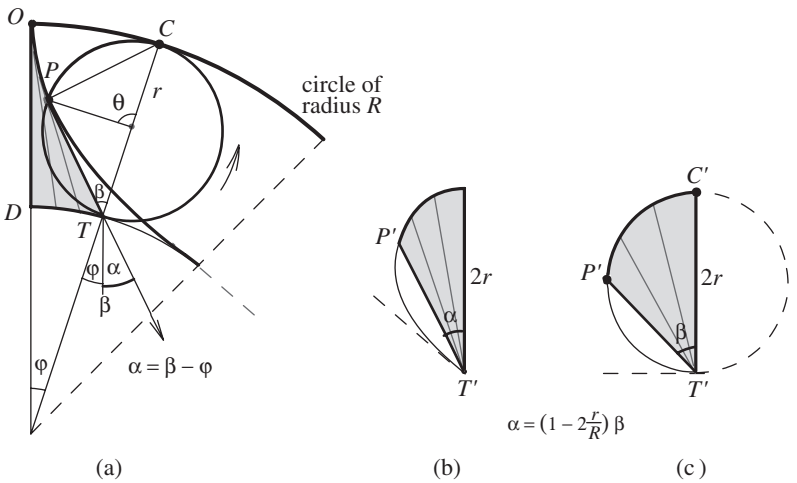

Figure 11. Proof of Lemma 2 for a hypocycloidal sector.

Proof of Theorem 2. We adapt the notation of Section 3 to Figure 9. Then Theorem 2 states that

$$[\text{Sector}] = \omega_+[\text{Segm}]. \tag{10}$$

But $[\text{Sector}] = [\text{Tusk}] + [\text{Segm}]$, and $\omega_+ = \kappa_+ + 2$, so (10) is equivalent to

$$[\text{Tusk}] = (\kappa_+ + 1)[\text{Segm}]. \tag{11}$$

To prove (11), refer to Figure 9a, and use Lemma 2 and (3) to get

$$[\text{Tusk}] = [\text{Ring}] - [\text{Cap}] - [\text{Wedge}] = [\text{Ring}] - (\kappa_+ + 1)([\text{Segm}] + [\text{Tri}]). \tag{12}$$

Here [Ring] is the area of portion $ODTC$ of the annular ring between the circles of radii R and $R + 2r$. On the other hand, $[\text{Ring}] = 2\varphi r(R + r) = 2r^2\theta(1 + r/R) = [\text{Rect}](\kappa_+ + 1)/2$ by (7) and (5), where $[\text{Rect}] = 2r^2\theta$ is the area of rectangle $OCTD$ in Figure 3. From (5) we find

$$[\text{Ring}] = (\kappa_+ + 1)(2[\text{Segm}] + [\text{Tri}]).$$

Use this in the right-hand side of (12) to obtain (11). But (11) is equivalent to (10), so this proves Theorem 2 for the epicycloid.

The same analysis based on Figure 11 works for the hypocycloid with the factors $\kappa_- = 1 - 2r/R$ and $\omega_- = 2 + \kappa_-$, because in this case $\alpha = \beta - \varphi$. ∎

Area of full cap and full arch. When rolling disk D of area $[D]$ makes one complete rotation, the cycloidal, epicycloidal, or hypocycloidal sector fills a region we call a *full arch.* The corresponding cycloidal cap fills a region we call a *full cap*. From Lemma 2 and Theorem 2 we obtain:

Corollary 1. *For any epicycloid the area of a full cap is $\kappa_+[D]$ and the area of a full arch is $\omega_+[D]$. For a hypocycloid the respective areas are $\kappa_-[D]$ and $\omega_-[D]$, and for a cycloid they are $[D]$ and $3[D]$, where $\kappa_\pm = 1 \pm 2r/R$, $\omega_\pm = \kappa_\pm + 2 = 3 \pm 2r/R$.*

Apparently no one has previously investigated the area of a cycloidal cap, but the result for a full arch is known. It is also derived in [**3**, Eq. (11)] by a different method (again without integration) in which both the rolling disk and the fixed circle are replaced by regular polygons.

The accompanying table gives values of r/R, $\kappa_\pm$, and $\omega_\pm$ for a few classical curves, including those in Figure 7. The first row relates to the cycloid, corresponding to $R = \infty$. The next two rows refer to two epicycloids with $\kappa_+ = 1 + 2r/R$: the cardioid ($r = R$), and the nephroid ($r = R/2$).

Curve	r/R	$\kappa_\pm$	$\omega_\pm$
Cycloid	0	1	3
Cardioid	1	3	5
Nephroid	1/2	2	4
Deltoid	1/3	1/3	7/3
Astroid	1/4	1/2	5/2
Diameter	1/2	0	2

The next two refer to two hypocycloids with $\kappa_- = 1 - 2r/R$: the deltoid ($r = R/3$), and the astroid ($r = R/4$). The last entry, a hypocycloid with $r = R/2$, may seem unusual: the hypocycloid is the diameter of the fixed circle. The region between the arch and the fixed circle of radius R is a semicircular disk of area $2\pi r^2$, half that of the fixed circle.

The table also illustrates a property common to all types of cycloids that follows directly from Corollary 1:

Corollary 2. *For any cycloid, epicycloid, or hypocycloid, the area of one full arch exceeds that of one full cap by twice the area of the rolling disk.*

Examples are shown in Figure 12, where in each case the darker shaded region is the full arch and the lighter shaded region is a full cap. The difference in shaded areas is

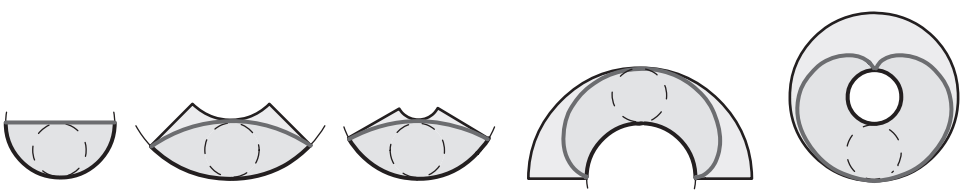

Figure 12. Difference of areas of shaded regions is twice the area of the rolling disks.

twice that of the rolling disk. If this general property could be established in a simpler way, then finding the areas of a full arch and a full cap would be almost trivial, because their sum is simply the area of a rectangle or annular ring.

Another interesting property is inherited from the fact that $\omega_+ + \omega_- = 6$. For any epicycloid obtained by a disk of radius r rolling outside a fixed circle of radius R, there is a corresponding hypocycloid obtained by a disk of the same radius r rolling inside, and we call the two cycloidal curves *complementary*. When the outside disk and the inside disk turn through the same angle θ, Theorem 2 tells us that *the sum of the areas of the complementary sectors in Figure 8 is six times that of the overlapping circular segment cut from the rolling disk by chord PC, regardless of R.* This implies the following property of the combined area of complementary full arches.

Corollary 3. *The sum of the areas of one full arch of an epicycloid and its complementary hypocycloid is equal to six times the area of the rolling disk.*

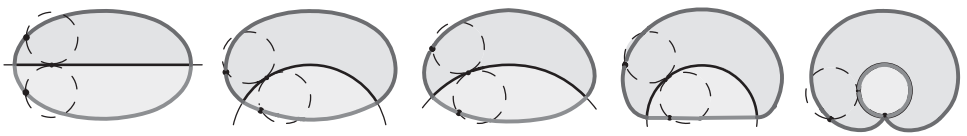

Figure 13. All combined regions have the same area: six times the area of the rolling disk.

Examples are shown in Figure 13 with various values of R, but with rolling disk of given radius r. In each case the sum of the darker and lighter shaded areas is six times that of the rolling disk. Incidentally, their difference is $(4r/R)[D]$.

5. AREAS OF CYCLOIDAL RADIAL AND ORDINATE SETS. The area of an epicycloidal radial set (darker shading in Figure 14a) can be calculated by standard

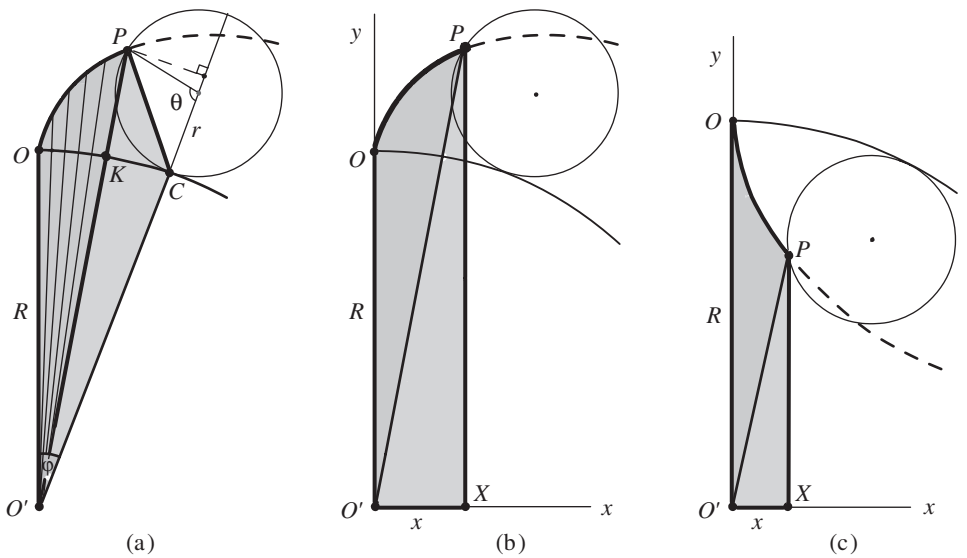

Figure 14. Geometric determination of the area of (a) epicycloidal radial set $O'OP$, (b) epicycloidal ordinate set $O'OPX$, and (c) hypocycloidal radial and ordinate sets.

integration techniques based on a polar equation for the tracing point P involving parameter θ of the rolling disk. The calculations are lengthy and the resulting formula is extremely complicated. This section shows how to find this area as a simple consequence of Theorem 2, avoiding polar equations and integration.

Consider the epicycloidal radial set $O'OP$ in Figure 14a. It is bounded by two radial segments $O'O$, $O'P$, and epicycloidal arc OP. Denote its area by [Radial]. Then we have

$$[\text{Radial}] = [OPC] + [O'OC] - [O'PC], \tag{13}$$

where $[OPC]$ is the area of epicycloidal sector OPC, $[O'OC]$ is the area of circular sector $O'OC$, and $[O'PC]$ the area of triangle $O'PC$. Theorem 2 tells us that $[OPC] = \omega_+[\text{Segm}]$, where $\omega_+ = 3 + 2r/R$ and [Segm] is given by (6). Also, $[O'OC] = \frac{1}{2}R^2\varphi = \frac{1}{2}Rr\theta$, and $[O'PC] = \frac{1}{2}Rr\sin\theta$; hence (13) can be written in the form

$$[\text{Radial}] = \left(\frac{R}{r} + \omega_+\right)[\text{Segm}]. \tag{14}$$

A corresponding formula holds for the area of a hypocycloidal radial set. Both results are contained in the following theorem:

Theorem 3. *The area of an epicycloidal or hypocycloidal radial set is given by*

$$[\text{Radial}] = \left(\frac{R}{r} \pm \omega_\pm\right)[\text{Segm}] = \left(\frac{R}{r} + 2\frac{r}{R} \pm 3\right)\frac{r^2}{2}(\theta - \sin\theta), \tag{15}$$

with the + sign for the epicycloid, and the − sign for the hypocycloid.

Now we can easily find the area [Ordinate] of ordinate set $O'OPX$ in Figure 14b or 14c by adding the area of right triangle $O'XP$ to that of epicycloidal or hypocycloidal radial set $O'OP$:

Theorem 4. *The area of an epicycloidal or hypocycloidal ordinate set is given by*

$$[\text{Ordinate}] = \left(\frac{R}{r} \pm \omega_\pm\right)[\text{Segm}] + \frac{1}{2}xy \tag{16}$$

with the + sign for the epicycloid, and the − sign for the hypocycloid.

In (16), x and y are the rectangular coordinates of P with respect to origin O' in Figure 14b or 14c. They are given in terms of parameter θ by the well-known equations (which can be derived directly from Figure 14):

$$x = (R \pm r)\sin\frac{r\theta}{R} - r\sin\left(1 \pm \frac{r}{R}\right)\theta, \qquad y = (R \pm r)\cos\frac{r\theta}{R} \mp r\cos\left(1 \pm \frac{r}{R}\right)\theta.$$

Here the upper sign is used for the epicycloid and the lower sign for the hypocycloid. The area of ordinate set $O'OPX$ can also be calculated directly by integration, using these parametric equations. The calculation is tedious and leads to a lengthy unpleasant formula, in contrast to compact and geometrically revealing formula (16).

As $R \to \infty$ in Figure 14b, vertical segments OO' and PX remain parallel, and the portion of the region $O'OPX$ outside the circle of radius R becomes the shaded region

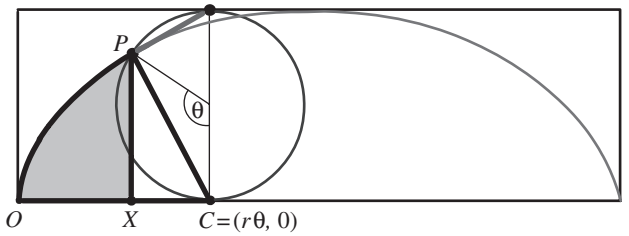

Figure 15. Cycloidal sector *OPC* is the union of ordinate set *OXP* and triangle *CXP*.

shown in Figure 15. This is the ordinate set of a cycloid, whose area we denote by $A(\theta)$. It is usually calculated by integration, using parametric equations for the cycloid.

We can also calculate $A(\theta)$ by a limiting argument based on (15) or (16), involving an indeterminate form of the type $\infty - \infty$. But we prefer to determine $A(\theta)$ directly and more simply from Theorem 1, avoiding parametric equations, integration, and indeterminate forms. To do so, note that in Figure 15 area $A(\theta)$ equals the area of cycloidal sector *OPC* minus the area $[CXP]$ of right triangle *CXP*. Hence by Theorem 1 we have

$$A(\theta) = 3[\text{Segm}] - [CXP].$$

In terms of angle of rotation θ and the coordinates (x, y) of point P, we have $[CXP] = \frac{1}{2}y(r\theta - x)$, and [Segm] is given by (6).

6. CONCLUDING REMARKS. Cycloidal curves have been investigated since ancient times. Epicycloids were used by Apollonius around 200 BC and by Ptolemy around 200 AD to describe the apparent motion of planets. The rich and interesting history of cycloids and their connections to many classical problems is well documented in [**5**], including early efforts by Galileo, Torricelli, Mersenne, Roberval, and others to determine the area of the cycloidal arch in Figure 1. Despite a large literature that exists on cycloidal curves, the new area properties stated in this article seem to have escaped notice, even though simple geometric proofs can be given without integral calculus and even without equations representing the curves. The key ideas of this paper exploit the use of normals and tangents which, in turn, lead naturally to applications of Mamikon's sweeping-tangent theorem. Surprisingly, the main results regarding areas of general cycloidal caps and sectors, as well as both radial and ordinate sets, are expressed directly in terms of the area of a wedge or of a segment of the rolling disk. We were pleased to observe that for the ordinary cycloid, throughout the entire process of rolling the disk, the area ratios [Cap]/[Wedge], [Tusk]/[Segm], [Sector]/[Segm] are the integers 1, 2, 3, respectively.

Three charming contributions to the history of cycloidal quadrature, made by Huygens, Leibniz, and Johannis Bernoulli, are closely related to our Lemma 1. In the tradition of Archimedes, they were seeking special portions of cycloidal regions whose areas are those of simple rectilinear shapes. Figure 16 illustrates their common setting. Each cycloidal arch is circumscribed by a rectangle bisected by a horizontal center line, with the rolling circle placed at its center.

In 1658, Huygens showed that the cycloidal segment cut off by the dashed line in Figure 16a, which bisects the upper half of the rectangle, has area equal to half that of the regular hexagon inscribed in the circle, or, equivalently, equal to the area of the shaded equilateral triangle adjacent to the segment.

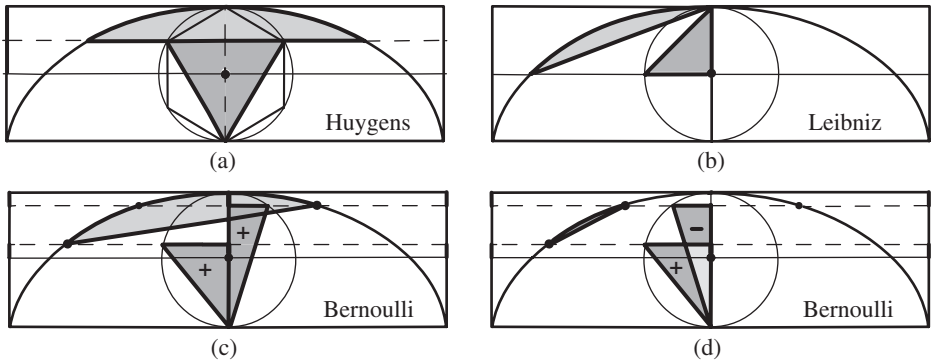

Figure 16. Quadrature of special cycloidal segments by Huygens, Leibniz, and Bernoulli.

Two decades later, in 1678, Leibniz showed that the cycloidal segment in Figure 16b has the same area as the shaded right triangle whose legs are radii of the circle.

After another two decades, in 1699, Bernoulli extended both these results, using two horizontal dashed lines equidistant from the upper and central lines in Figure 16a and b. He demonstrated that the area of the cycloidal segment in Figure 16c is the sum of the areas of the two shaded right triangles, while that of the smaller cycloidal segment in Figure 16d is the difference of the triangular areas, and then he deduced the results of Huygens and Leibniz as corollaries. Incidentally, the diagram in Figure 16c appears on the title pages of all four volumes of Bernoulli's collected works.

Inspired by these examples, we consider a segment cut from a general point of a cycloid to its highest point. In Figure 17a, the general point is lower than the center line, and the segmental area is the sum of the areas of the two shaded right triangles. In Figure 17b, the general point is above the center line and the segmental area is the difference of the triangular areas. By combining two such segments with the triangle between them, and using intricate dissections, we can deduce the area of a general cycloidal segment in Figure 17c, and in particular Bernoulli's special segments, both of whose endpoints are above the center line.

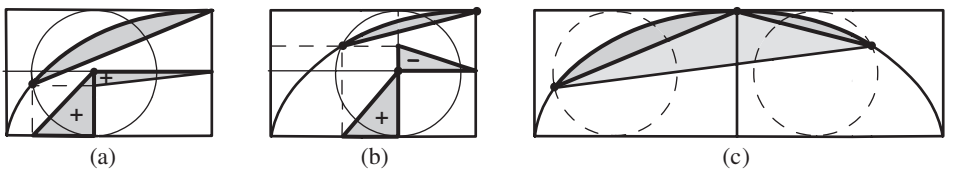

Figure 17. The area of a cycloidal segment is the sum of the areas of the shaded triangles in (a), and the difference of areas in (b). General cycloidal segment in (c) obtained from types in (a) and (b).

Now we outline the argument relating the foregoing to our Lemma 1, which we illustrate in a companion form in Figure 18a: the area of the cycloidal tail (tangent sweep) is equal to that of the adjacent circular segment (tangent cluster).

Figure 18b shows the cycloidal segment of Figure 17a inscribed in a triangle whose horizontal base s equals the length of the adjacent circular arc. Using the fact that the cycloidal tail and the circular segment have equal areas, it is a simple exercise to deduce the area relations in Figure 17a. In a similar manner we get the result in Figure 17b. Bernoulli's results also follow directly from Figure 18a.

Finally, in Figure 19, we include our own special cycloidal quadrature relation: the shaded curvilinear region and the shaded square have equal areas.

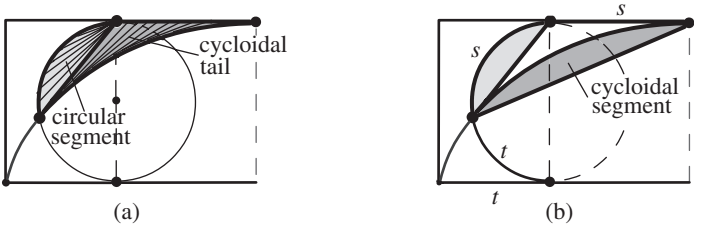

Figure 18. (a) Circular segment and cycloidal tail have equal areas. (b) Cycloidal tail and cycloidal segment form a triangle.

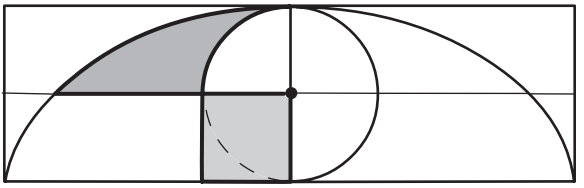

Figure 19. The shaded curvilinear region has the same area as the square.

When the rolling circle has unit radius, the quadratures in Figures 16a, b, and 19 are even more attractive because each curvilinear region has the same area as a polygonal region whose area is an algebraic number. By contrast, the area of a full cycloidal arch traced by a unit circle is 3π, which is not algebraic.

7. APPENDIX. For ease of reference, this appendix briefly describes Mamikon's sweeping-tangent theorem. Figure 20 shows a piecewise smooth curve τ. As a tangent vector (whose length may vary) moves continuously along τ, it sweeps out a region called a *tangent sweep*. When each tangent vector is translated, parallel to itself, to bring the points of tangency together at a single point, the set of translated segments is called a *tangent cluster.* A rotated version of this cluster (with the same area) can be formed by translating each tangent vector from τ so that the free-end points of the tangent vectors are brought to a common point. In this article we use the rotated cluster.

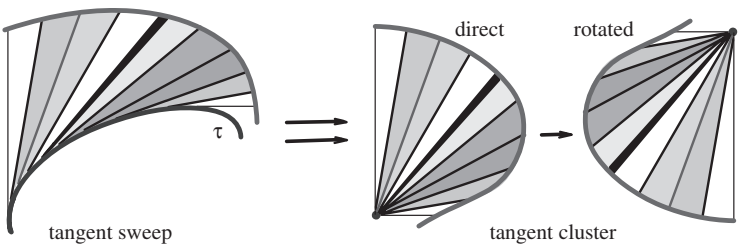

Figure 20. Tangent sweep and its corresponding tangent cluster have equal areas.

Mamikon's sweeping-tangent theorem. *The area of a tangent sweep is equal to the area of its tangent cluster, regardless of the curve* τ.

1. T. M. Apostol, A visual approach to calculus problems, *Engineering and Science* **LXIII** (2000) 22–31. Also available at: http://www.its.caltech.edu/~mamikon/calculus.html, which also contains animations demonstrating the use of Mamikon's sweeping-tangent theorem.
2. T. M. Apostol and M. A. Mnatsakanian, Tangents and subtangents used to calculate areas, this MONTHLY **109** (2002) 900–908.
3. ———, Generalized cyclogons, *Math Horizons* September (2002) 25–28.
4. M. A. Mnatsakanian, On the area of a region on a developable surface, *Doklad. Armenian Acad. Sci.* **73** (1981) 97–101 (Russian); communicated by Academician V. A. Ambartsumian.
5. J. J. O'Connor and E. F. Robertson, MacTutor History of Mathematics Archive, "Cycloid" (1997), available at: http://www-groups.dcs.st-and.ac.uk/~history/Curves/Cycloid.html.

TOM M. APOSTOL joined the Caltech mathematics faculty in 1950 and became professor emeritus in 1992. He is director of Project MATHEMATICS! (http://www.projectmathematics.com), an award-winning series of videos he initiated in 1987. His long career in mathematics is described in the September 1997 issue of the *College Mathematics Journal*. He is currently working with colleague Mamikon Mnatsakanian to produce materials demonstrating Mamikon's innovative and exciting approach to mathematics.
California Institute of Technology, 253-37 Caltech, Pasadena, CA 91125
apostol@caltech.edu

MAMIKON A. MNATSAKANIAN received a Ph.D. in physics in 1969 from Yerevan University, where he became professor of astrophysics. As an undergraduate he began developing innovative geometric methods for solving many calculus problems by a dynamic and visual approach that makes no use of formulas. He is currently working with Tom Apostol under the auspices of Project MATHEMATICS! to present his methods in a multimedia format.
California Institute of Technology, 253-37 Caltech, Pasadena, CA 91125
mamikon@caltech.edu

Mathematics Is . . .

"Mathematics is persistent intellectual honesty."

Moses Richardson, Mathematics and intellectual honesty, this MONTHLY **59** (1952) 73.

—Submitted by Carl C. Gaither, Killeen, TX